Dynamic structure factors and Lyapunov modes in disordered chains

Kai Helbig,[1,*] Wolfram Just,[2,†] Günter Radons,[1] and Hongliu Yang[1]
[1]*Institute of Physics, Chemnitz University of Technology, 09107 Chemnitz, Germany*
[2]*School of Mathematical Sciences, Queen Mary, University of London, Mile End Road, London E1 4NS, United Kingdom*
(Received 15 March 2010; published 13 August 2010)

We investigate various dynamic structure factors for harmonic and anharmonic chains. For harmonic chains with mass disorder we find some unexpected features, such as a fine structure contributing to a central peak, which is present also in the spatial spectra of the eigenfunctions. These results are contrasted with structure factors of Lyapunov modes obtained for the disordered Lennard-Jones chain. For this nonlinear system the static and the dynamic Lyapunov structure factors show opposite trends in their temperature dependence.

DOI: 10.1103/PhysRevE.82.026206 PACS number(s): 05.45.−a, 05.70.Ln, 63.50.−x

I. INTRODUCTION

In recent years dynamical systems theory has contributed to a considerable extent toward the understanding of the foundations of statistical mechanics. Particular aspects concern the understanding of fluctuations in equilibrium and nonequilibrium systems [1], or the link between transport coefficients and properties of the underlying dynamical system [2,3]. In addition, the concept of sensitivity, Lyapunov exponents, and corresponding Lyapunov modes has been explored in molecular dynamics simulations, to uncover a new view on hydrodynamic behavior [4–6].

Here we are concerned with properties of the fluctuations of a density

$$\rho_w(x,t) = \sum_{\nu=0}^{N-1} w_\nu \delta(x - q_\nu(t)) \tag{1}$$

in simple dynamical systems. Depending on the nature of the weights w_ν given to the particles with index ν at positions q_ν, an expression like Eq. (1) describes, for instance in molecular hydrodynamics, number density, mass density, or current density [7]. In the context of Lyapunov analysis the weights w_ν correspond to components of the Lyapunov vectors. Fluctuations of such densities are usually captured by the two point autocorrelation function

$$C_w(x-x',t-t') = \langle \rho_w(x,t)\rho_w(x',t')\rangle, \tag{2}$$

where the (canonical) average $\langle \ldots \rangle$ may contain, e.g., a spatial average as well in order to restore translation invariance if a system of finite extent is considered. Quantities such as the correlation function (2) and, in particular, its spatiotemporal Fourier transform $S_w(k,\omega)$

$$S_w(k,\omega) = \frac{1}{2\pi}\int dt e^{i\omega t}\frac{1}{N}\sum_{\nu,\nu'}\langle w_\nu w_{\nu'} e^{ikq_\nu(t)}e^{-ikq_{\nu'}(0)}\rangle \tag{3}$$

and its static counterpart, given by

$$S_w(k) = \int d\omega S_w(k,\omega) \tag{4}$$

play a central role for the physics of fluids, solids, and disordered systems, from a theoretical as well as an experimental point of view [7]. For instance, such quantities are at the heart of quantifying the glass transition [8,9].

One of our goals is the investigation of densities which are derived from the internal nonlinear dynamics of the system. Lyapunov exponents and the corresponding Lyapunov modes are one of the most important quantifiers for the sensitivity and chaos in a dynamical system [4–6,10,11]. For one-dimensional Hamiltonian systems with N degrees of freedom, Lyapunov modes are vectors with components $\{[\delta p_\nu^{(\alpha)}(t), \delta q_\nu^{(\alpha)}(t)], \nu=0,\ldots,N-1\}$ which characterize perturbations of momenta and coordinates of reference trajectories in phase space. The growth rate is given by the corresponding Lyapunov exponents $\lambda^{(\alpha)}$, where we label by $\alpha=1,\ldots,2N$ the exponents in decreasing order. It is known that the time dependence of these modes is governed solely by the time dependence of the reference trajectory $\{(p_\nu(t),q_\nu(t)), \nu=0,\ldots,N-1\}$ [12]. Lyapunov modes, corresponding to exponents which are small in modulus, show hydrodynamic behavior in extended dynamical systems when, for instance, translational symmetry prevails [6]. Thus, it is tempting to study densities where the weights w_ν are given by the corresponding components $w_\nu = \delta q_\nu^{(\alpha)}(t)$ of the αth Lyapunov mode [4,5]. The time translation invariance expressed in Eq. (2) is still valid because the time dependence of the weights is also governed by the Liouville operator. In systems with spatial translational symmetry some modes corresponding to Lyapunov exponents $\lambda^{(\alpha_0)}=0$ associated with translational invariance are constant in time and independent of the particle index ν, i.e., $[\delta p_\nu^{(\alpha_0)}(t), \delta q_\nu^{(\alpha_0)}(t)]=(0,c)$ [4,6,13]. If the mode number α corresponds to the index of such a Goldstone mode α_0 [14] the dynamic Lyapunov structure factor $S^{(\alpha)}(k,\omega)$ with $w_\nu = \delta q_\nu^{(\alpha)}(t)$ is proportional to the ordinary dynamic structure factor $S_\varrho(k,\omega)$ ($w_\nu=1$). This is one motivation for studying ordinary dynamic structure factors as reference quantities for the more general Lyapunov structure factors. As we aim at a comparison of both quantities we restrict the current analysis to Lyapunov structure factors where the weights are derived from the spatial components of the Lyapunov vectors.

*Present address: Institute of Nuclear and Particle Physics, TU Dresden, 01062 Dresden, Germany.
†w.just@qmul.ac.uk

Our main focus here is on simple spatially one-dimensional systems in order to investigate properties of generalized dynamic structure factors from a dynamical systems point of view. Of course, results already exist in the literature, e.g., a classical investigation of the effect of randomness on the dynamic structure factor [15], or testing mode-coupling theories in simple models [16]. There has been renewed interest in those topics motivated by the treatment of nontrivial lattice structures [17] and by fundamental problems of glassy systems [18]. However, since even for the very simple harmonic system no closed analytical form for the dynamic structure factor can be written down, detailed investigations were not possible without resorting to numerical computations or first order expansions, i.e., in the one-excitation approximation. Despite the renewed interest in simple model systems, it is surprising that the classic dynamic structure factor of the harmonic chain with disorder has not been investigated in detail.

Here, we present an analysis of generalized dynamic structure factors for simple one-dimensional models. Section IV is concerned with harmonic chains and isotopic mass disorder. For comparison Sec. III reviews such a model with a periodic structure. While for harmonic chains parts of the analysis can be done by analytical means (cf., e.g., the appendixes) models with nonlinear interaction forces require the application of molecular dynamics. In that context Lyapunov modes play, of course, a nontrivial role. Section V presents the discussion of a disordered chain with Lennard-Jones interaction. We focus here in particular on a comparison between the (classic) dynamic structure factor and a structure factor derived from hydrodynamic Lyapunov modes. For the determination of the modes we resort here to an orthogonal set, i.e., we employ the standard Wolf algorithm for the computation [19]. Some computational aspects are summarized in Sec. II, while the conclusion contains a discussion of the findings and a selection of open problems.

II. MODEL SYSTEMS AND COMPUTATIONAL ISSUES

We will consider chains of N particles with masses $m_0, m_1, \ldots, m_{N-1}$ which are coupled by pair interactions. Two different types of systems will be considered. The first model is the simple harmonic chain with nearest neighbor interaction where the Hamiltonian reads

$$H_{harm} = \sum_{\nu} \frac{p_\nu^2}{2m_\nu} + \frac{g}{2}\sum_{\nu} (q_{\nu+1} - q_\nu - d)^2. \tag{5}$$

The ground state of the system is given by the configuration $q_\nu = \nu d$, $\nu = 0, \ldots N-1$ where $L=Nd$ denotes the length of the chain. Depending on the boundary condition the potential may contain additional terms which are not stated in Eq. (5) explicitly. Several boundary conditions will be discussed in the subsequent sections namely, (i) periodic boundary conditions $q_\nu = q_{\nu+N}$, (ii) fixed boundary conditions $q_{-1}=0$ and $q_N=0$, and chains with (iii) open boundaries.

The second class of model we are going to consider is a one-dimensional Lennard-Jones fluid

$$H_{LJ} = \sum_{\nu} \frac{p_\nu^2}{2m_\nu} + \sum_{\nu \neq \mu} U(|q_\mu - q_\nu|), \tag{6}$$

where the interaction is mediated by the standard (truncated) 6–12 potential

$$U(r) = \begin{cases} 4\varepsilon\left(\left(\frac{\sigma}{r}\right)^{12} - \left(\frac{\sigma}{r}\right)^{6}\right) + U_{cut} & \text{if } 0 < r \leq 2.5\sigma \\ 0 & \text{else} \end{cases}, \tag{7}$$

where the constant U_{cut} ensures for continuity at $r=2.5\sigma$. As usual the parameter σ determines the position of the minimum of the potential at $r_{\min} = 2^{1/6}\sigma$. If L denotes the length of the chain and $d=L/N$ the average distance of particles, then a meaningful dimensionless density parameter is given by $\rho = r_{\min}/d$. For most parts of our investigations we will focus on the case $\rho=1$, i.e., a system with nondegenerate ground state where all particles are essentially located in adjacent minima of the potential.

The computation of the dynamic structure factor for the harmonic chain can be done partially by analytical means. The main numerical task consists of diagonalizing the coupling matrix and computing related spectral sums (cf. Appendix A for some details). Thus, systems of considerable size can be treated even for models with a random mass distribution. In our numerical investigations we use harmonic chains with $N=1000$ particles. A system of finite size shows temporal recurrences, which for harmonic chains are of order N. To avoid such finite-size effects Fourier transforms have been restricted to a finite time interval of length $T \sim N\sqrt{\bar{m}/g}$, with $\bar{m}$ being the average mass. The resulting spectrum is smoothed by a Hann window, i.e., a weighted average over neighboring frequency bins with weights 1/4, 1/2, and 1/4. For fixed boundary conditions the recurrence time increases by a factor four compared to systems with periodic boundary conditions. Furthermore, fixed boundaries eliminate any Goldstone mode.

The case of the Lennard-Jones fluid has to be treated differently as the canonical average cannot be computed by analytical means. Thus, one has to resort to molecular dynamics simulations which, in our case, limits the system size to $N=200$ particles. The averages in Eqs. (2) and (3) are now understood as microcanonical averages, which are calculated numerically via averaging over time. The numerical integration is performed by the standard velocity Verlet algorithm with step size $10^{-4}\sqrt{48\bar{m}\sigma^2/\varepsilon}$. For preparing a state with given temperature we choose random initial conditions in configuration space and momenta according to a Boltzmann distribution with temperature β^{-1} in momentum space. The momenta are redistributed according to the Boltzmann distribution after 10^4 time steps and the process is repeated 100 times. After thermalization the fluctuations in kinetic energy, i.e., in temperature are less than 1%. For the computation of the Lyapunov spectrum and the Lyapunov vectors we use the standard Gram-Schmidt reorthogonalization algorithm [19]. Vectors are reorthogonalised each 1500th time step. We allow 10^7 time steps for the vectors to align along their intrinsic directions. We then choose a time span of 4×10^7 for the

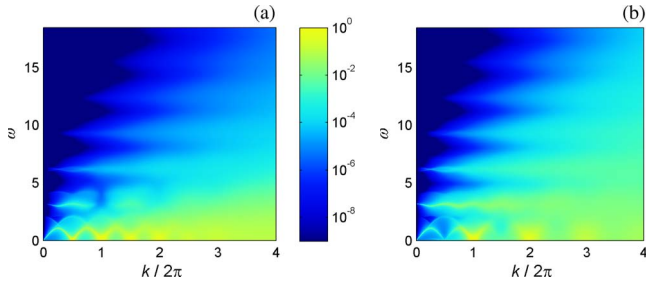

FIG. 1. (Color online) Dynamic structure factors of a harmonic chain of alternating masses with ratio of 8:1, temperature $\beta=100$, and periodic boundary conditions: (a) mass density $[S_m(k,\omega)$, weights $w_\nu=m_\nu]$, (b) number density $[S_\varrho(k,\omega)$, weights $w_\nu=1]$. If not stated otherwise, the same color coding is used in the other figures.

actual numerical computation of the dynamic structure factor using normalized Lyapunov vectors. All the other numerical issues are treated along the lines of the harmonic chain.

Finally, to get some more insight into the analytical structure Appendix B contains a brief discussion of the accuracy of one-phonon approximations, in particular, within the context of the harmonic chain where exact results beyond plain numerical simulations are available.

III. HARMONIC CHAIN WITH ALTERNATING MASSES

We consider a chain of particles with alternating masses m_0 and m_1. Given the analytical expressions derived for the harmonic chain [cf., e.g., Eqs. (A1) in Appendix A] it is natural to measure the wave number k in units of $1/d$ and the inverse temperature β in units of $1/gd^2$. There are several but equivalent choices for a time scale. If we denote by $\bar{m}=(m_0+m_1)/2$ the average mass per particle, the dimensionless frequency ω is measured in units of $\sqrt{g/\bar{m}}$. Accordingly, the dynamic structure factor will be rescaled by such a time scale. In addition, the structure factor derived from the mass density will be rescaled by $\bar{m}^2$ as well.

Let us first focus on a brief comparison of the dynamic structure factors $S_\varrho(k,\omega)$ and $S_m(k,\omega)$ for the number density and the mass density, respectively. Figure 1 contains results for a system with periodic boundary conditions and a mass ratio $m_0/m_1=8:1$. On a large scale the results are quite similar. In both cases the dispersion relation with acoustic and optical branch is visible. In addition, higher harmonics occur as well which are caused by the nonlinear dependence of the structure factor on the phonon amplitudes. These higher order branches cause a comb-like structure. Such structures and the optical branch are more pronounced when the number density is considered. On the one hand, the optical branch derived from the structure factor of the mass density shows minima in the intensity at about integer values of $k/(2\pi)$. On the other hand, the acoustic branch for the number density seems to develop similar minima at half-integer values.

Figure 2 illustrates the influence of different boundary conditions on the dynamic structure factor. As one would expect the result does not show a strong dependence on the boundary condition. However, except for periodic boundary conditions the structure factor displays some dispersionless intensities [near $\omega\approx 1.2$ and $\omega\approx 1.7$ in Fig. 2(b), and at $\omega=1.5$ in Fig. 2(c)]. Such structures relate to surface or evanescent modes, i.e., exponentially localized eigenmodes of the finite-size system. For open boundary conditions they appear only, if a light particle is located at least at one of the boundaries. These modes, of course, do not show up in a system with periodic boundary conditions. In addition, the system with open boundary conditions displays a central low frequency peak which is related to fluctuations of the system size. Many features just described are quite well captured by standard one-phonon approximations (cf., e.g., Fig. 13 in Appendix B).

So far we have considered a single value for the temperature. In fact, no qualitatively new features appear when changing the temperature of the system. The dispersion branches become blurred when temperature is increased, i.e., linewidths increase. For high temperatures, i.e., for $\beta<10$, the dispersion branches are not visible any longer beyond the first Brillouin zone. If the temperature is around $\beta^{-1}=1$ the average kinetic energy is so large that all but the linear dispersion $\omega=c\cdot k$ for very low k values has disappeared, signaling the speed of sound in the hot fluid. For even higher temperatures the structure factor of noninteracting particles is approached.

IV. HARMONIC CHAIN WITH BINARY MASS DISORDER

In order to discuss the impact of disorder we now analyze a diatomic harmonic chain where particles with masses m_0

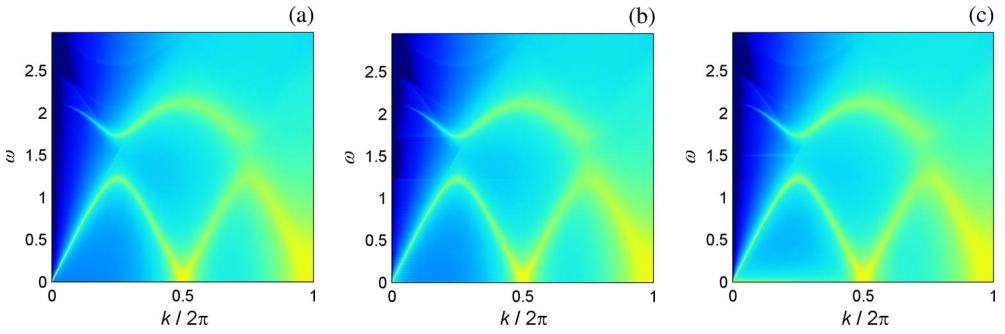

FIG. 2. (Color online) Mass density dynamic structure factor $S_m(k,\omega)$ of harmonic chains of alternating masses for a mass ratio of 2:1, inverse temperature $\beta=100$, and different boundary conditions: (a) periodic, (b) fixed, (c) open. Note the appearance of a central peak $(\omega=0)$ in (c).

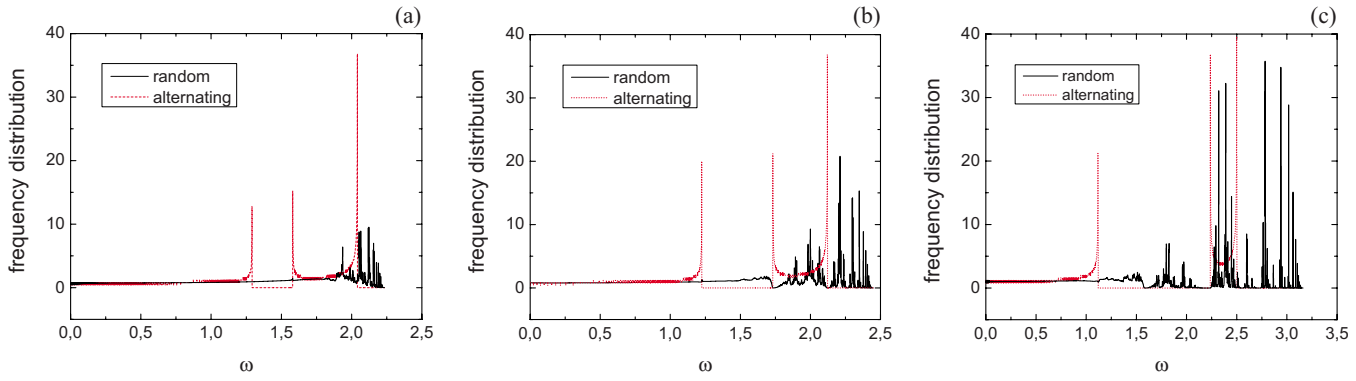

FIG. 3. (Color online) Density of states for a harmonic chain with binary isotopic disorder for three different mass ratios m_0/m_1: (a) 3:2, (b) 2:1, (c) 4:1. Data have been obtained from averaging over 100 000 random permutations of a chain of length $N=5000$, with different masses to occur with equal probability. The dotted red line shows for comparison the density of states of the corresponding periodic chain.

and m_1 take random positions. For simplicity we confine to situations where both types of particles appear in equal numbers. The study of such systems, in particular, with regards to spectral properties, is of course a classical subject [20,21]. Here we just briefly mention some features which are relevant in our context. Figure 3 shows the density of states for three different mass ratios m_0/m_1. It is in fact well known that the density of states tends toward a smooth distribution for mass ratios smaller than 2:1, while the distribution shows irregular behavior at higher frequencies for larger mass ratios [22]. As expected, the high frequency component is related with a localization phenomenon for the corresponding eigenmodes [23]. One expects such signatures to show up again in the dynamic structure factor.

We have seen in the previous section that boundary conditions play a minor role for the computation of the dynamic structure factor in a finite-size system. This is even more the case for random chains because of the inhomogeneities stemming from the disorder. We therefore focus on systems with fixed boundary conditions. For the dynamic structure factor we take an average over ten realizations of the disorder as such a value seems to be a reasonable compromise between numerical effort and the accuracy of the resulting graphs.

Figure 4 first compares data below and above the critical mass ratio 2:1. For a subcritical mass ratio the structure factor displays a well defined smooth dispersion relation as one would expect for a system with a continuous density of states. The actual shape of the dispersion relation is qualitatively similar to a monoatomic chain. For a critical mass ratio and beyond, the smooth dispersion relation still exists for low frequencies but pronounced gaps appear at larger frequencies in accordance with the structure of the density of states (cf. Fig. 3). In both cases, sub- and supercritical, the dynamic structure factor for the mass density displays a central peak at $\omega=0$ as well.

Unlike a chain with periodic mass distribution the random system shows a substantial change when instead of the mass density the number density is considered. Figures 4(c) and 5(b) display for comparison also the number density structure factor $S_\varrho(k,\omega)$ for a supercritical mass ratio 4:1. In contrast to the mass density structure factor $S_m(k,\omega)$ the central frequency peak is significantly reduced for $S_\varrho(k,\omega)$. On the other hand the higher frequency localized modes are more pronounced when the structure factor is based on the number density.

Let us have a closer look at the central peak which occurs at $\omega=0$ for the mass structure factor. The numerical data can be fitted quite well by a Lorentzian (cf. Fig. 6) over quite a wide range of wave numbers. For very large wave numbers the central peak broadens and interferes with other structures of $S_m(k,\omega)$.

From the Lorentzian line shape the linewidth and the spectral weight can be evaluated quantitatively (cf. Fig. 7). The linewidth shows a quadratic dependence on the wave

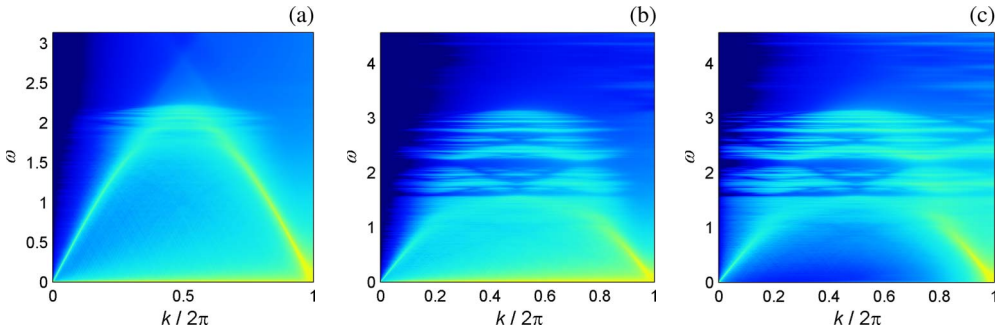

FIG. 4. (Color online) Mass density structure factor $S_m(k,\omega)$ of a binary disordered harmonic chain at inverse temperature $\beta=1000$ for mass ratios (a) 3:2 (subcritical), (b) 4:1 (supercritical, cf. Figure 3) and (c) number density structure factor $S_\varrho(k,\omega)$ for mass ratio 4:1. The data have been averaged over a sample of ten realizations.

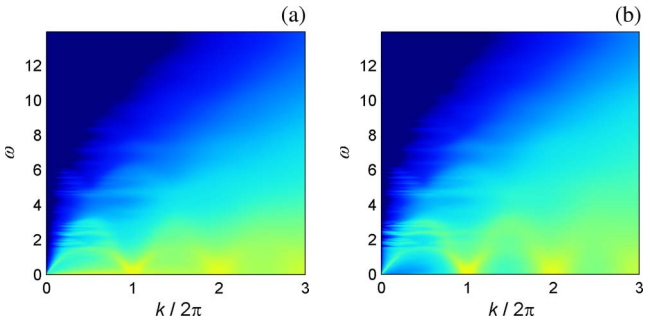

FIG. 5. (Color online) Dynamic structure factor of a binary disordered harmonic chain of masses with ratio 4:1 and temperature $\beta=100$: (a) structure factor computed from the mass density, (b) structure factor computed from the number density.

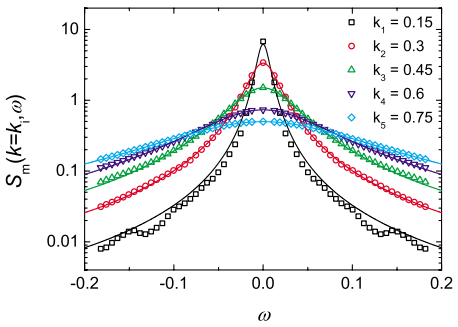

FIG. 6. (Color online) Central peak in the mass structure factor as a function of the wavenumber. Symbols correspond to cross sections of the data shown in Fig. 5(a), lines are numerical fits with a Lorentzian.

number while the spectral weight is essentially independent of k. Some deviations are visible at integer values of $k/(2\pi)$, which can be attributed to interference with the dispersion relation of the random system. Overall the observed dependence of the central peak on frequency and wave number can be expressed as

$$S_m(k,\omega) \sim (\alpha k)^2/((\alpha k)^4 + \omega^2). \tag{8}$$

Such an analytic expression points toward a diffusive process [7,24]. The central peak is strongly reduced when the number density structure factor $S_\varrho(k,\omega)$ is considered, a fact which is plausible because $S_\varrho(k,\omega)$ is by definition less sensitive to mass density fluctuations which, e.g., are caused by permutations of particles with different masses.

To gain a deeper insight into the nature of this central peak, we compare the averaged structure factor from Fig. 4(b) with that of a single realization of mass disorder (cf. Fig. 8). It is clear that the continuous peak in Fig. 4(b) has strong contributions from the superposition of many dispersion branches starting at k-values, which depend on the actual disorder realization [cf. Fig. 8(b)]. Due to averaging with respect to these realizations, or due to self averaging [25] in the infinite volume limit of one realization, this fine structure is smoothed out.

Interestingly this fine structure can already be detected in the spatial power spectrum of the eigenmodes if ordered by the eigenfrequency (see Fig. 9).

The fine structure appears also for other boundary conditions. To our knowledge the appearance of this fine structure in $S_\varrho(k,\omega)$, $S_m(k,\omega)$, and in the eigenfunctions of the disordered harmonic chain has not been realized before. Note, however, that similar fine structures had been observed also in harmonic Fibonacci chains [17]. In both cases such structures correspond to phonon branches of various unit cells approximating the quasi-periodic or random sequence of particles. For the random chains, at variance with the quasi-periodic system with its long-ranged correlations, we do not have a systematic build-up of structures as the system size is increased. As can be seen from Fig. 9 such a mechanism would result in a smooth profile in the thermodynamic limit. Obviously this is one contribution to the intensity of the central peak observed for the random chain.

V. LENNARD-JONES FLUID WITH BINARY MASS DISORDER

So far we have considered systems with harmonic interactions where the dynamic structure factor can be evaluated, at least to some extent, analytically. We now focus on a chain of particles with a Lennard-Jones-type interaction [cf. Eqs.

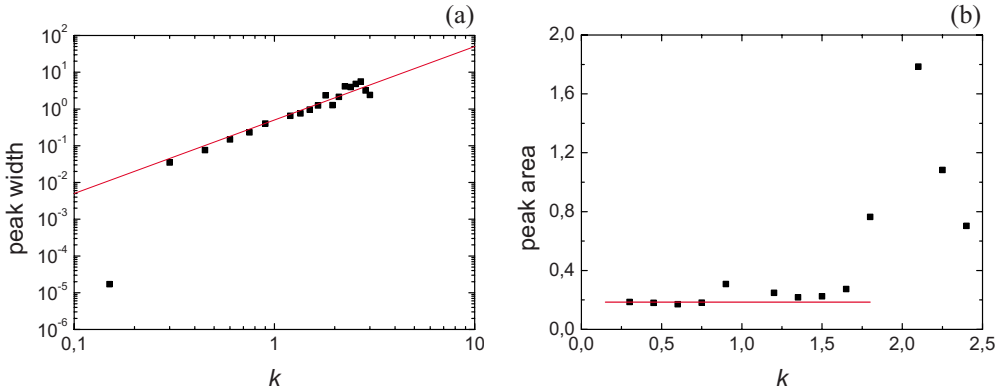

FIG. 7. (Color online) Linewidth and spectral weight of the central peak as a function of the wave number [cf. Figs. 5(a) and 6]. The straight lines correspond to least square fits for low wave numbers with slope two and zero, respectively.

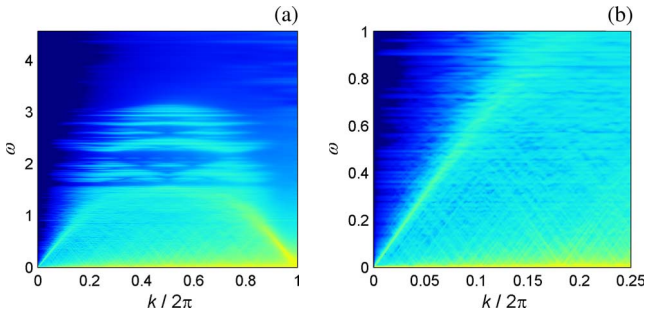

FIG. 8. (Color online) (a) Mass structure factor of a binary disordered harmonic chain of $N=1000$ particles at inverse temperature $\beta=1000$ with mass ratio 4:1 for a single disorder realization [cf. 4(b) for an average over 10 realizations]. (b) Detailed view of the fine structure for small wave numbers.

(6) and (7)] where the correlation functions have to be evaluated by molecular dynamics. Since the potential contains a hard core repulsion the order of the particles is, in contrast to the harmonic case, strictly preserved within the spatially one-dimensional set up used here. Results for monoatomic chains and its dynamical anomalies can be found in [26,27]. To compare with the results of the previous sections we consider here a random mass configuration where particles with masses m_0 and m_1 occur with equal probability.

We will focus on cases where the density $\rho=r_{\min}/d=2^{1/6}\sigma\cdot N/L$ [see Eq. (7)] takes the value one. We measure the inverse temperature β in units of $1/\varepsilon$ and the wave number k in units of $1/d$. The frequency ω is measured in units of $\sqrt{\varepsilon/(48\bar{m}\sigma^2)}$.

Here we concentrate on the mass density dynamic structure factor $S_m(k,\omega)$ because it contains more information compared to the number density dynamic structure factor. In addition, due to the nonlinear nature of the system, it now becomes important to consider also the dynamic structure factor of the Lyapunov modes. We found recently that in a diatomic chain of coupled maps, under the influence of mass differences, the Lyapunov spectra and vectors split into acoustic and optical branches [28]. Such a similarity to the phonon case in response to mass discrepancies indicates a possible relation between phonons and Lyapunov modes in respect of representing collective motions of a high dimensional system. We therefore investigate in some detail the Lyapunov structure factor as well. The corresponding weights w_ν in Eq. (3) are time dependent and we use a temporal average in Eq. (2) to restore time translation invariance. From the computational point of view we evaluate the spatial Fourier transform of the density $\rho_w(k,t)$, Eq. (1), and compute the structure factor as the absolute value of the temporal Fourier transform, applying the Wiener-Khinchin theorem. In that respect the chaotic dynamics of the nonlinear system accelerates the speed of converge of thermodynamic averages. Two kinds of Lyapunov structure factors, dynamic ones $S^{(\alpha)}(k,\omega)$ and its frequency integral Eq. (4), the static ones, will be compared with the mass dynamic structure factors $S_m(k,\omega)$.

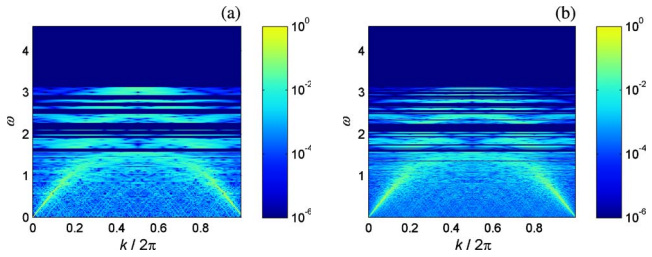

FIG. 9. (Color online) Spatial power spectrum of the eigenmodes as function of the eigenfrequencies for a binary disordered chain of (a) $N=200$ and (b) $N=1000$ particles (periodic boundary conditions, mass ratio 4:1).

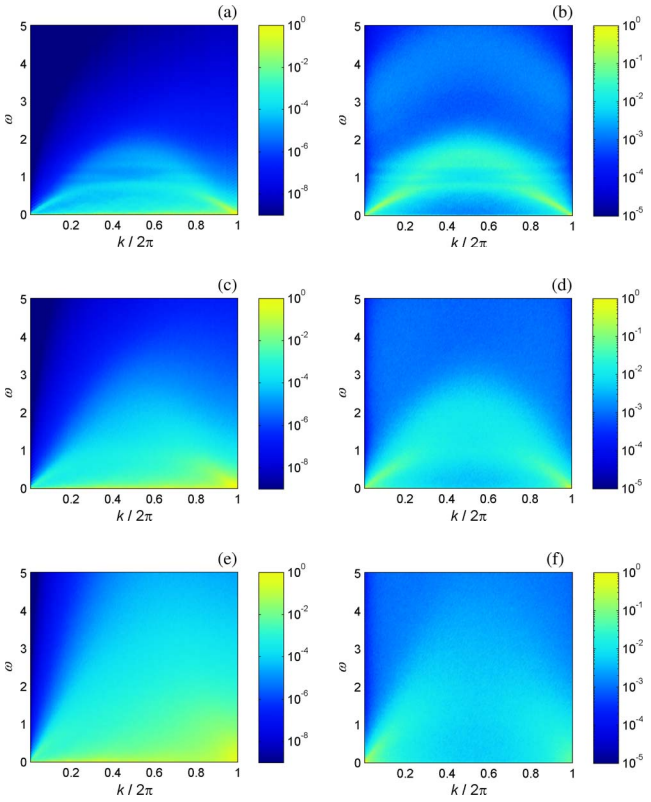

FIG. 10. (Color online) Dynamic structure factors of a Lennard-Jones chain of $N=200$ particles with binary disordered masses with ratio 4:1, density $\rho=1$, and increasing temperatures: (a,c,e) dynamical structure factor of the mass density, (b,d,f) dynamical Lyapunov structure factor for mode number 196. Inverse temperatures: (a,b) $\beta=100$, (c,d) $\beta=10$, and (e,f) $\beta=1$.

Figure 10 shows a comparison between the mass dynamic structure factor and the dynamic Lyapunov structure factor for different temperatures, density $\rho=1$, and mass ratio $m_0/m_1=4:1$. For the latter structure factor we have chosen a Lyapunov mode with mode number $\alpha=196$ in a system with $N=200$ particles, i.e., 400 modes. Such a mode corresponds to a small but positive Lyapunov exponent as the mode number is close to the center of the Lyapunov spectrum where the exponent vanishes because of symmetries. One expects such a mode to be relevant for the hydrodynamic properties of the dynamic system as the corresponding Lyapunov exponent is small in modulus [4,5].

For low temperatures, say $\beta\geq 10$, the dispersion relations are clearly visible in the dynamic structure factor and in the dynamic Lyapunov structure factor (Fig. 10). For the latter

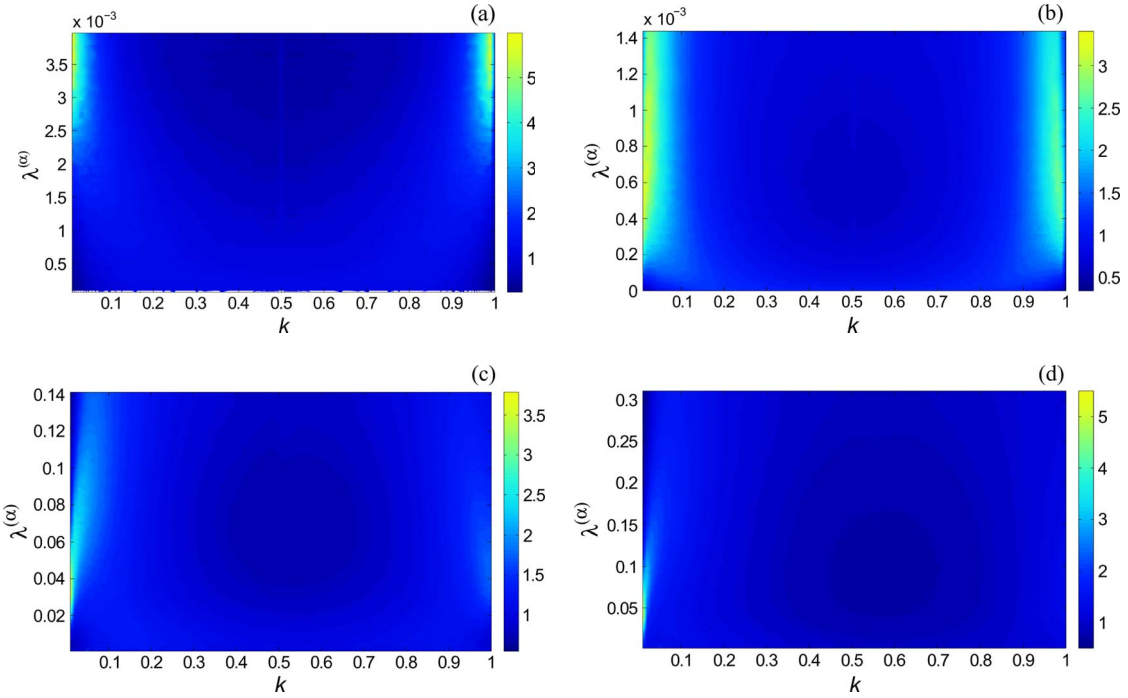

FIG. 11. (Color online) Static Lyapunov structure factors of a Lennard-Jones chain of $N=200$ particles with binary disordered masses with ratio 4:1, density $\rho=1$, and increasing temperatures. Inverse temperatures: (a) $\beta=100$, (b) $\beta=10$, (c) $\beta=1$ and (d) $\beta=0.1$ (cf. as well Fig. 12 for a detailed view).

the dispersion relation is even more pronounced and the spatial structures are better defined for small length scales. The structure factors are qualitatively similar to the harmonic chain (cf., e.g., Fig. 5). However, the slope of the dispersion relations at low wave numbers shows a dependence on the temperature which is not surprising for the ordinary dynamic structure factor, since in a nonlinear system one expects the speed of sound to depend slightly on the temperature. The slopes obtained from least square fits of the dynamic structure factor and of the dynamic Lyapunov structure factor shown in Fig. 10 read (a) 3.41 ± 0.02 and (b) 3.51 ± 0.02 ($\beta=100$), (c) 3.75 ± 0.02 and (d) 4.19 ± 0.05 ($\beta=10$), and (e) 6.43 ± 0.02, and (f) 5.80 ± 0.2 ($\beta=1$).

Most significantly, there does not appear a central peak in the dynamic Lyapunov structure factor contrary to the dynamic structure factor based on the mass density. Furthermore, the dynamic Lyapunov structure factor seems to be a symmetric function for wavenumbers $0 \leq k \leq 2\pi$. For high temperatures, say $\beta=1$ [see Fig. 10(f)], where the kinetic energy per particle becomes comparable in size to the potential energy, the dispersion branches disappear because of large linewidths. In addition, the dynamic Lyapunov structure factor loses its symmetry and becomes featureless, as is also true in general for very high k-values. All these features do not seem to depend strongly on the mass ratio.

Figure 11 shows the static Lyapunov structure factor for different temperatures, the same density and mass ratio as in Fig. 10, and for different mode number, i.e., as a function of the Lyapunov exponent. Such a feature adds an additional facet to our analysis. Compared to the dynamic structure factor and dynamic Lyapunov structure factors, a different tendency of temperature dependence can be clearly seen from the figure. For low temperature, say $\beta=100$ and $\beta=10$, no dispersion relation can be identified from the static Lyapunov structure factors. With increasing temperature a linear λ-k dispersion emerges gradually, as can be seen from Figs. 11 and 12. The observed difference in the temperature dependence can be intuitively understood in the following way: the frequency ω in dynamic (Lyapunov) structure factors represents an oscillating feature which characterizes the harmonic part of the system dynamics, while the Lyapunov exponent λ represents a typical expansion time scale which characterizes the complementary anharmonic, chaotic part of the system dynamics. With increasing temperature, the anharmonicity of the system dynamics is enhanced which leads to the gradual emergence of a linear λ-k dispersion in the static Lyapunov structure factors. With decreasing temperature the system dynamics approaches the harmonic limit and therefore the ω-k dispersion becomes more pronounced in the dynamic (Lyapunov) structure factors. Further investigations are required to uncover a quantitative relation between the two dispersion relations.

VI. CONCLUSION AND DISCUSSION

Dynamic structure factors probe for the density excitations in particle systems. Thus, properties of such correlation functions may depend strongly on the special density under consideration. Such an aspect can be already illustrated by the harmonic chain as seen in Sec. IV, where the intensity of the low frequency peak depends on whether the mass or the number density has been considered. We therefore concluded that in the present context the peak is partially related to the diffusive motion of localized mass excitations.

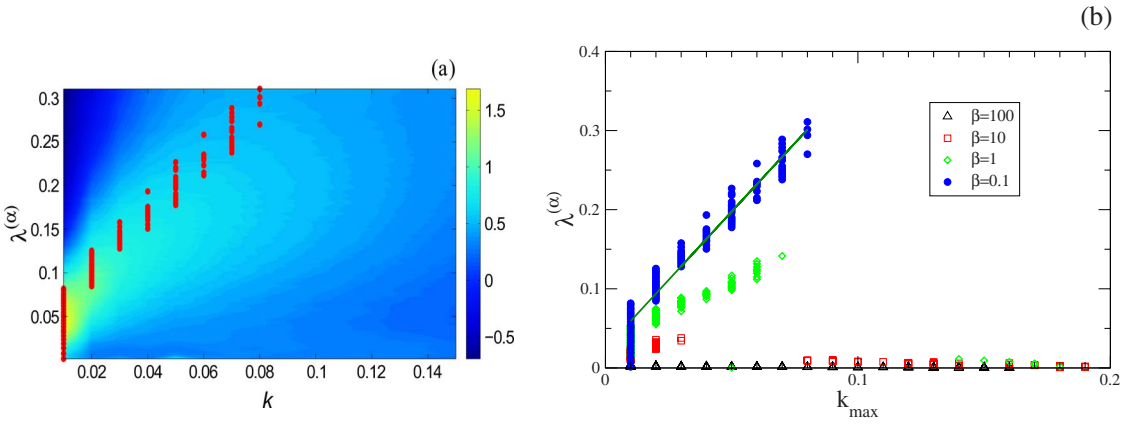

FIG. 12. (Color online) (a) Static Lyapunov structure factor and (b) λ-k dispersion relation of a Lennard-Jones chain of $N=200$ particles, with binary disordered masses with ratio 4:1 and density $\rho=1$. Note that (a) is an enlargement of the panel (d) of Fig. 11 to show the linear dispersion.

The concept of a Lyapunov structure function is able to uncover completely new aspects in random nonlinear systems. Such a structure factor behaves differently compared to the more traditional concepts as can be seen, e.g., from the unexpected symmetry properties computed in Sec. V. However, to judge the relevance of Lyapunov densities, further systematic large scale simulations are required. For instance, the dependence of the dynamic Lyapunov structure factor on the Lyapunov mode number in the hydrodynamic regime has to be investigated further. The Wolf algorithm used in the determination of the Lyapunov modes yields an orthogonal basis in the relevant subspaces and the algorithm is relatively easy to apply. But such modes are normally different from the covariant splitting in dynamical systems. Recently, efficient algorithms have been developed to estimate the covariant basis system [29] but such algorithms are computationally still quite demanding.

To proceed even further, analytical investigations of simple linear systems could be useful. For instance, one could address the relevance of Lyapunov modes within the context of harmonic disordered chains with moderate numerical efforts. It would be tempting to explore whether closed analytical expressions can be derived. At least the application of straightforward one-phonon approximations might be appropriate tools to capture the essentials of the corresponding dynamic structure factor. Furthermore, one could focus on other integrable system, like the Toda chain, where it is likely that analytical expression for the dynamic structure factor might be accessible. In addition, such models could reveal the relevance of different types of excitations, i.e., plane waves and solitons, for the Lyapunov density fluctuations. With regards to disordered Lennard-Jones chains we concentrated here on the case with density $\rho=1$. Such a value is special in the sense that the zero temperature equilibrium positions of the particles are close to the minima of the interaction potential. A systematic study of the density dependence, although numerically quite demanding, seems to be tempting, in particular, since a change in density may trigger degeneracies of the ground state. Altogether, the Lyapunov structure factor is likely to be a useful tool to get further insight into how dynamical systems theory can contribute to the foundations of nonequilibrium statistical mechanics.

ACKNOWLEDGMENT

We thank Christian Drobniewski for helpful discussions. The authors gratefully acknowledge support by DFG (Grant No. RA 416/6-2) and by DAAD.

APPENDIX A: HARMONIC CHAIN

The spatial Fourier transform of the density correlation function (2) yields the intermediate scattering function $F_w(k,t)$. For systems which violate translation invariance, e.g., for the case of non-periodic boundary conditions, we consider an additional spatial average so that $F_w(k,t)$ is defined by

$$F_w(k,t) = \frac{1}{N}\sum_{\nu,\mu} w_\nu w_\mu \exp(ik(\nu-\mu)d) \times \exp\{-k^2\langle[u_\nu(t)-u_\mu]^2\rangle/2\}. \tag{A1}$$

Here $u_\nu = q_\nu - \nu d$ denotes the deviation of the particle from its ground state position, and we have used the fact that such a variable is normally distributed when the average $\langle\ldots\rangle$ with respect to the canonical ensemble is considered. The temporal correlation functions which appear in the exponent can be evaluated easily using the linear equations of motion.

Using vector notation $\underline{u}=(u_0,u_1,\ldots,u_{N-1})^T$ and $\underline{p}=(p_0,p_1,\ldots,p_{N-1})^T$ the equations of motion determined by the Hamiltonian (5) read

$$\dot{\underline{u}}(t) = \underline{\underline{M}}^{-1}\underline{p}(t), \quad \dot{\underline{p}}(t) = -\underline{\underline{G}}\underline{u}(t), \tag{A2}$$

where $M_{\nu\mu}=m_\nu\delta_{\nu,\mu}$ denotes the diagonal inertia matrix and

$$G_{\nu\mu} = g[2\delta_{\nu,\mu} - \delta_{\nu,\mu-1} - \delta_{\nu,\mu+1} + \kappa(\delta_{0,0}+\delta_{N-1,N-1}) + \chi(\delta_{0,N-1}+\delta_{N-1,0})] \tag{A3}$$

abbreviates the matrix of the force constants. Its precise form depends on the chosen boundary conditions, i.e.,

$$\kappa = \begin{cases} -1 & \text{open} \\ 0 & \text{fixed, periodic} \end{cases}, \quad \chi = \begin{cases} -1 & \text{periodic} \\ 0 & \text{fixed, open} \end{cases}. \tag{A4}$$

With the standard transformation

$$\underline{\tilde{u}} = \underline{\underline{M}}^{1/2}\underline{u}, \quad \underline{\tilde{p}} = \underline{\underline{M}}^{-1/2}\underline{p}, \quad \underline{\underline{\tilde{G}}} = \underline{\underline{M}}^{-1/2}\underline{\underline{G}}\underline{\underline{M}}^{-1/2} \tag{A5}$$

one can cast Eq. (A2) in normal form

$$\dot{\underline{\tilde{u}}}(t) = \underline{\tilde{p}}(t), \quad \dot{\underline{\tilde{p}}}(t) = -\underline{\underline{\tilde{G}}}\underline{\tilde{u}}(t). \tag{A6}$$

The positive semi-definite matrix of the force constants can be diagonalized by an orthogonal transformation $\underline{\underline{Q}}$

$$\underline{\underline{\tilde{G}}} = \underline{\underline{Q}}^T\underline{\underline{\Omega}}^2\underline{\underline{Q}}, \tag{A7}$$

where the diagonal matrix $\Omega_{\nu\mu}=\omega_\nu\delta_{\nu,\mu}$ contains the eigenfrequencies of the system. Thus, integration of Eq. (A6) becomes a trivial task and the solution reads

$$\underline{u}(t) = \underline{\underline{M}}^{-1/2}\underline{\underline{Q}}^T(\cos(\underline{\underline{\Omega}}t)\underline{\underline{Q}}\underline{\tilde{u}} + \underline{\underline{\Omega}}^{-1}\sin(\underline{\underline{\Omega}}t)\underline{\underline{Q}}\underline{\tilde{p}}). \tag{A8}$$

For systems with periodic or open boundary conditions the total momentum is preserved and the frequency matrix contains a vanishing eigenvalue. In such a case the Moore-Penrose pseudo inverse for $\underline{\underline{\Omega}}^{-1}$ has to be considered as such a choice corresponds to a center of mass coordinate system. This matrix solution has been introduced in [30] for the case of fixed boundary conditions.

The computation of the correlation function in Eq. (A1)

$$\langle (u_\nu(t)-u_\mu)^2\rangle = \langle u_\nu^2\rangle + \langle u_\mu^2\rangle - 2\langle u_\nu(t)u_\mu\rangle \tag{A9}$$

is now straightforward. The normal coordinates $(\underline{\underline{Q}}\underline{\tilde{u}})_\nu$ and $(\underline{\underline{Q}}\underline{\tilde{p}})_\mu$ are independent Gaussian variables with zero mean and variances $1/(\beta\omega_\nu^2)$ and $1/\beta$, respectively [cf., e.g., Eq. (A6) and the Hamiltonian (5)]. Thus, the expression (A8) yields for $t=0$

$$\langle u_\nu^2\rangle = \sum_\lambda \frac{[(\underline{\underline{M}}^{-1/2}\underline{\underline{Q}}^T)_{\nu\lambda}]^2}{\beta\omega_\lambda^2} = \frac{(\underline{\underline{G}}^{-1})_{\nu\nu}}{\beta}, \tag{A10}$$

where we have used the identity

$$\sum_\lambda \frac{(\underline{\underline{M}}^{-1/2}\underline{\underline{Q}}^T)_{\nu\lambda}(\underline{\underline{M}}^{-1/2}\underline{\underline{Q}}^T)_{\mu\lambda}}{\omega_\rho^2} = (\underline{\underline{M}}^{-1/2}\underline{\underline{Q}}^T\underline{\underline{\Omega}}^{-2}\underline{\underline{Q}}\underline{\underline{M}}^{-1/2})_{\nu\mu} = (\underline{\underline{G}}^{-1})_{\nu\mu}, \tag{A11}$$

which follows immediately from the definitions (A5) and (A7). For the time-dependent part of Eq. (A9) we obtain by a similar reasoning

$$\langle u_\nu(t)u_\mu\rangle = \sum_\lambda \frac{(\underline{\underline{M}}^{-1/2}\underline{\underline{Q}}^T)_{\nu\lambda}(\underline{\underline{M}}^{-1/2}\underline{\underline{Q}}^T)_{\mu\lambda}}{\beta\omega_\lambda^2}\cos(\omega_\lambda t) = \frac{(\underline{\underline{G}}^{-1})_{\nu\mu}}{\beta} - 2\sum_\lambda \frac{(\underline{\underline{M}}^{-1/2}\underline{\underline{Q}}^T)_{\nu\lambda}(\underline{\underline{M}}^{-1/2}\underline{\underline{Q}}^T)_{\mu\lambda}}{\beta\omega_\lambda^2} \times \sin^2(\omega_\lambda t/2). \tag{A12}$$

Combining Eqs. (A10) and (A12) we arrive at the final result

$$\langle (u_\nu(t)-u_\mu)^2\rangle = \frac{1}{\beta}\left((\underline{\underline{G}}^{-1})_{\nu\nu} + (\underline{\underline{G}}^{-1})_{\mu\mu} - 2(\underline{\underline{G}}^{-1})_{\nu\mu} + \frac{4}{\sqrt{m_\nu m_\mu}}\sum_\lambda Q_{\lambda\nu}\frac{\sin^2(\omega_\lambda t/2)}{\omega_\lambda^2}Q_{\lambda\mu}\right). \tag{A13}$$

As already stated above, for periodic and open boundary conditions the pseudoinverse of the frequency matrix has to be adopted, i.e., vanishing frequencies have to be excluded from the sum. Equations (A1) and (A13) constitute the result for the intermediate scattering function. Evaluation just requires the (numerical) diagonalization of the rescaled interaction matrix, cf. Eq. (A7). The dynamic structure factor is then obtained by Fourier transformation. Of course, for simple mass configurations further simplification of the expression is possible.

For the static case, i.e., for the static structure factor $F_w(k,0)$, just the stationary correlation enters. That expression depends on the interaction only

$$\langle (u_\nu - u_\mu)^2\rangle = \frac{1}{\beta}[(\underline{\underline{G}}^{-1})_{\nu\nu} + (\underline{\underline{G}}^{-1})_{\mu\mu} - 2(\underline{\underline{G}}^{-1})_{\nu\mu}] \tag{A14}$$

as one expects to be the case for a classical thermodynamic average since phase space integrals factorize. Thus, any mass disorder does not affect the static structure factor. The static correlation (A14) can be easily evaluated from Eq. (A3) for different boundary conditions

$$\langle (u_\nu - u_\mu)^2\rangle = \frac{|\nu-\mu|}{\beta g} \times \begin{cases} 1 & \text{open} \\ 1-|\nu-\mu|/N & \text{periodic} \\ 1-|\nu-\mu|/(N+1) & \text{fixed} \end{cases}. \tag{A15}$$

Therefore, the static structure factor for constant weights can even be evaluated in closed analytical form.

APPENDIX B: ONE-PHONON APPROXIMATIONS

Even for the harmonic chain the intermediate scattering function (A1) is anharmonic since the amplitude correlation function appears in the exponent, due to the nonlinear dependence of the density [Eq. (1)] on coordinates. For analytical purposes one may use expansions in terms of amplitude correlations, i.e., in terms of Fourier amplitudes. We will estimate the accuracy of such standard first order expansions within our setup.

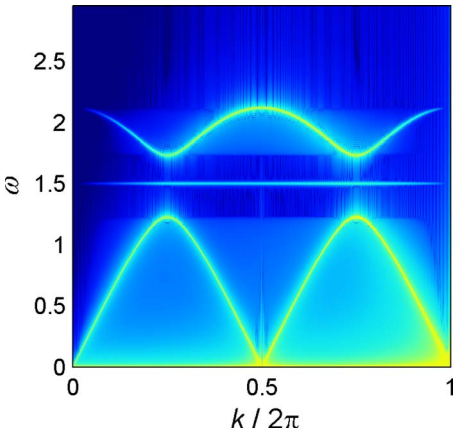

FIG. 13. (Color online) Debye-Waller approximation for the dynamic structure factor of a harmonic chain of alternating masses with ratio 2:1, temperature $\beta=100$, and open boundary conditions [cf. Eq. (B5)]. The approximation yields finite values only for frequencies covered by the dispersion relation and the eigenmode in the spectral gap is clearly visible [cf. Fig. 2(c) for the exact result].

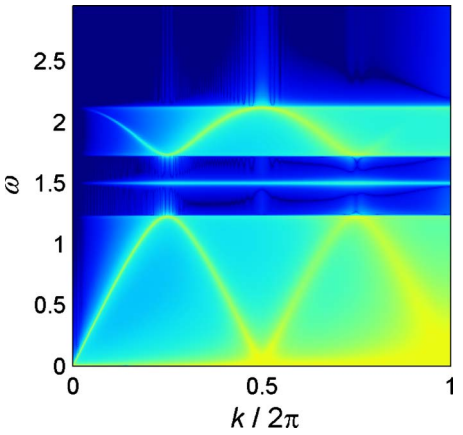

FIG. 14. (Color online) Static approximation for the dynamic structure factor of a harmonic chain of alternating masses with ratio 2:1, temperature $\beta=100$, and open boundary conditions [cf. Eq. (B7)]. The approximation yields finite values only for frequencies covered by the dispersion relation and the eigenmode in the spectral gap is clearly visible [cf. Fig. 2(c) for the exact result].

There are in fact different ways to implement such an expansion. One may expand in such a way that the leading term reproduces the Debye-Waller factor

$$\exp(-k^2\langle(u_\nu(t)-u_\mu)^2\rangle/2) = \exp(-k^2(\langle(u_\nu^2\rangle+\langle u_\mu^2\rangle)/2)(1+k^2\langle u_\nu(t)u_\mu\rangle+\cdots). \tag{B1}$$

If we just focus on a first order, i.e., on a one-phonon approximation, the time-dependent part of the intermediate scattering function (A1) reads

$$F_w^{(DW)}(k,t)=\frac{k^2}{N}\sum_{\nu,\mu} w_\nu w_\mu \exp(ik(\nu-\mu)d)\exp(-k^2/2(\langle u_\nu^2\rangle + \langle u_\mu^2\rangle))\langle u_\nu(t)u_\mu\rangle. \tag{B2}$$

Using Eq. (A12) such an approximation may be simplified further

$$F_w^{(DW)}(k,t)=\frac{k^2}{\beta N d^2}\sum_\lambda \frac{|\xi_\lambda(k)|^2}{\omega_\lambda^2}\cos(\omega_\lambda t), \tag{B3}$$

where

$$\xi_\lambda(k)=d\sum_\nu \frac{w_\nu}{\sqrt{m_\nu}}\exp(ikd\nu-k^2\langle u_\nu^2\rangle)Q_{\lambda\nu} \tag{B4}$$

denotes the spatial Fourier transform of the appropriate eigenmode of the system. Performing the Fourier transform (for a finite-size system with an appropriate regularisation) one obtains the dynamic structure factor in closed form

$$S_w^{(DW)}(k,\omega)=\frac{(k/\omega)^2}{2\pi\beta N d^2}\sum_\lambda \delta(\omega-\omega_\lambda)|\xi_\lambda(k)|^2. \tag{B5}$$

In order to get an estimate of the accuracy of the one-phonon approximation (B3) we compare such an expression with the numerically exact result discussed in Sec. III. Figure 13 shows the one-phonon approximation for a binary periodic harmonic chain with mass ratio 2:1. We have evaluated the sums for a system with finite size $N=1000$ and have computed the temporal Fourier transform numerically (see Sec. II for a few details). As the Debye-Waller factor diverges for a chain in the thermodynamic limit such contributions have been discarded when evaluating the sums in Eq. (B3). We obtain nonvanishing values, of course, only for frequencies covered by the dispersion relation. The dispersion relation itself is clearly reproduced but other aspects of the dynamic structure factor [cf. Fig. 2(c) for the numerical exact result] are hardly reproduced. In particular, most of the background structure visible in Fig. 13 seems to be due to the boundary conditions and thus should be largely considered to be a numerical artifact.

The previous one-phonon approximation may be improved when the expansion of the time-dependent exponential is performed in such a way that the exact static structure factor is recovered in leading order

$$\exp\{-k^2\langle[u_\nu(t)-u_\mu]^2\rangle/2\}=\exp[-k^2\langle(u_\nu-u_\mu)^2\rangle/2]\{1+k^2\langle[u_\nu(t)-u_\nu]u_\mu\rangle+\cdots\}. \tag{B6}$$

Then to first order the intermediate scattering function (A1) reads

$$\begin{aligned} F_w^{(S)}(k,t) &= F_w(k,0)+\frac{k^2}{N}\sum_{\nu\mu} w_\nu w_\mu \exp[ik(\nu-\mu)d] \\ &\quad\times\exp[-k^2\langle(u_\nu-u_\mu)^2\rangle/2]\langle[u_\nu(t)-u_\nu]u_\mu\rangle \\ &= F_w(k,0)-\frac{2k^2}{\beta N d^2}\sum_\lambda \Xi_\lambda \frac{\sin^2(\omega_\lambda t/2)}{\omega_\lambda^2} \end{aligned} \tag{B7}$$

when we use Eqs. (A10) and (A12) and the abbreviation

$$\Xi_\lambda = d^2 \sum_{\nu\mu} \left[\frac{w_\nu}{\sqrt{m_\nu}} \exp(ikd\nu) Q_{\lambda\nu} \right] \left[\frac{w_\mu}{\sqrt{m_\mu}} \exp(-ikd\mu) Q_{\lambda\mu} \right] \times \exp[-k^2 \langle (u_\nu - u_\mu)^2 \rangle / 2] \tag{B8}$$

which, apart from the contributions by the Debye-Waller factor, coincides with the intensity of the mode Eq. (B4). The result of such an approximation is shown in Fig. 14. Compared with the previous result and with the numerically exact data, Fig. 2(c), the approximation yields quite an improvement as now some structures beyond the linear dispersion branches are reproduced. Thus, it seems to be important that the one-phonon approximation preserves the correct static structure factor.

[1] G. Gallavotti and E. G. D. Cohen, Phys. Rev. Lett. **74**, 2694 (1995).
[2] D. J. Evans and G. P. Morris, *Statistical Mechanics of Nonequilibrium Liquids* (Academic Press, London, 1990).
[3] D. Ruelle, J. Stat. Phys. **95**, 393 (1999).
[4] G. Radons and H. L. Yang, e-print arXiv:nlin.CD/0404028; H. L. Yang and G. Radons, Phys. Rev. E **71**, 036211 (2005).
[5] H. L. Yang and G. Radons, Phys. Rev. Lett. **96**, 074101 (2006).
[6] C. Forster, R. Hirschl, H. A. Posch, and W. G. Hoover, Physica D **187**, 294 (2004).
[7] J. P. Hansen and I. R. McDonald, *Theory of Simple Liquids* (Academic Press, London, 1986).
[8] W. Götze and L. Sjögren, Rep. Prog. Phys. **55**, 241 (1992).
[9] R. Schilling and T. Scheidsteger, Phys. Rev. E **56**, 2932 (1997).
[10] J. P. Eckmann and D. Ruelle, Rev. Mod. Phys. **57**, 1115 (1985).
[11] H. A. Posch and R. Hirschl, in *Hard Ball Systems and the Lorentz Gas*, edited by D. Szász (Springer, Berlin, 2000), p. 279.
[12] S. V. Ershov and A. B. Potapov, Physica D **118**, 167 (1998).
[13] J.-P. Eckmann, C. Forster, H. A. Posch, and E. Zabey, J. Stat. Phys. **118**, 813 (2005).
[14] A. S. de Wijn and H. van Beijeren, Phys. Rev. E **70**, 016207 (2004).
[15] K. Kim and M. Nelkin, Phys. Rev. B **7**, 2762 (1973).
[16] G. Radons, J. Keller, and T. Geisel, Z. Phys. B **50**, 289 (1983).
[17] M. Engel, S. Sonntag, H. Lipp, and H.-R. Trebin, Phys. Rev. B **75**, 144203 (2007).
[18] M. Montagna, G. Ruocco, G. Viliani, R. Dell Anna, R. Di Leonardo, R. Dusi, G. Monaco, M. Sampoli, and T. Scopigno, Phys. Rev. Lett. **83**, 3450 (1999).
[19] A. Wolf, B. Swift, J. Swinney, and J. Vastano, Physica D **16**, 285 (1985).
[20] F. J. Dyson, Phys. Rev. **92**, 1331 (1953).
[21] Th. M. Nieuwenhuizen and J. M. Luck, J. Stat. Phys. **41**, 745 (1985).
[22] D. N. Payton and W. M. Visscher, Phys. Rev. **154**, 802 (1967).
[23] P. Dean, Rev. Mod. Phys. **44**, 127 (1972).
[24] H. L. Yang and G. Radons, Phys. Rev. E **73**, 016208 (2006).
[25] I. M. Lifshits, S. A. Gredeskul, and L. A. Pastur, *Introduction to the Theory of Disordered Systems* (Wiley, New York, 1988).
[26] S. Lepri, P. Sandro, and A. Politi, Eur. Phys. J. B **47**, 549 (2005).
[27] M. Bishop, J. Stat. Phys. **29**, 623 (1982).
[28] H. L. Yang and G. Radons, Phys. Rev. Lett. **99**, 164101 (2007).
[29] F. Ginelli, P. Poggi, A. Turchi, H. Chaté, R. Livi, and A. Politi, Phys. Rev. Lett. **99**, 130601 (2007).
[30] R. J. Rubin, Phys. Rev. **131**, 964 (1963).